

Effective three particle forces in polyvalent atoms

M. G. Kozlov^{1,2}, M. S. Safronova^{3,4}, S. G. Porsev^{1,3}, and I. I. Tupitsyn⁵

¹*Petersburg Nuclear Physics Institute, Gatchina 188300, Russia*

²*St. Petersburg Electrotechnical University "LETI",
Prof. Popov Str. 5, St. Petersburg, 197376, Russia*

³*Department of Physics and Astronomy, University of Delaware, Newark, Delaware 19716, USA*

⁴*Joint Quantum Institute, National Institute of Standards and Technology
and the University of Maryland, Gaithersburg, Maryland 20742, USA and*

⁵*Department of Physics, St. Petersburg State University,
Uljanovskaya 1, Petrodvorets, St. Petersburg, 198504, Russia*

(Dated: November 15, 2018)

We study effective three-particle interactions between valence electrons, which are induced by the core polarization. Such interactions are enhanced when valence orbitals have strong overlap with the outermost core shell, in particular for the systems with partially filled f -shell. We find that in certain cases the three-particle contributions are large, affecting the order of energy levels, and need to be included in high-precision calculations.

I. INTRODUCTION

Accurate prediction of atomic properties is crucial for many applications, ranging from tests of fundamental physics [1, 2] to building ultra-precise atomic clocks [3]. In recent years, atoms and ions with more complicated electronic structure, including lanthanides and actinides were in the focus of many studies [4–10]. In particular, highly-charged ions (HCI) with open nf -shells have been suggested for the design of high-precision atomic clocks and the search for the variation of the fine-structure constant [11, 12]. These applications require accurate predictions of transition wavelengths and other atomic properties, motivating further development of high-precision atomic methodologies.

It is well known that three-particle interactions play an important role in nuclear physics. Such interactions arise, for example, because of the internal structure of the nucleons, see Fig. 1.a. If the nucleon c polarizes the nucleon b , then interaction of the latter with the third nucleon a is modified. In atomic physics we deal with point-like electrons and such a mechanism of generating effective three-particle interactions is absent. However, atoms have an electronic shell structure and interactions between valence electrons are modified by the stronger bound core electrons, which form a kind of inhomogeneous dielectric medium. This is known as core polarization, or the screening effect and is described by the diagrams of the type of Fig. 1.b. The loop in this diagram includes the sums over all core states n and all possible states α above the core. However, some of the states α can be occupied by valence electrons and should be excluded due to the Pauli principle. This leads to the diagram Fig. 1.c, which cancels contributions of the states $\alpha = b, b'$ in the diagram Fig. 1.b. Therefore we can say that three-electron interactions (TEI) between valence electrons appear because core polarizability depends on the presence of the valence electrons. Note that TEI are also considered in condensed matter physics, see, e. g. [13].

The diagram Fig. 1.c (and its possible permutations)

is the only three-electron diagram in the second order of the many-body perturbation theory (MBPT) in residual two-electron interaction. In the case of initial three electron state (a, b, c) and final state (a', b', c') there are 36 diagrams, which differ by permutations of these states. This number rapidly grows with the number of valence electrons and the number of valence configurations, which are included in the calculation. As a result, the total contributions of such diagrams for polyvalent atoms may be large.

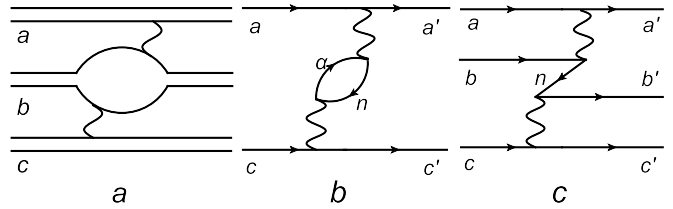


FIG. 1: Effective interactions. (a) Complex particles: the particle c polarizes the particle b , which then interacts with the particle a ; (b) Screened interaction: the particle c polarizes the core and interacts with the particle a ; (c) The particles a , b , and c interact through the excitation of the core.

Effective TEI described by the diagram Fig. 1.c were introduced in Ref. [14] within the CI+MBPT approach. This approach combines the configuration interaction (CI) method for treating valence correlations with MBPT for core-valence and core-core correlations. Since then this method was used for calculations of various properties of polyvalent atoms with several closed core shells [15–21]. Later, a CI+AO (all order) method was developed in [22–24]. It includes higher-order core valence correlations by combining configuration interaction and linearized coupled-cluster approach.

In Ref. [14] neutral Tl was calculated as a three-valence atom and TEI contribution to the valence energy was found to be very small, on the order of 10 cm^{-1} , leading to the omission of TEI contributions in a vast majority

of later calculations. The reason for the suppression of the TEI contribution is clear from Fig. 1.c: valence orbitals b and b' typically have very small overlap with all core orbitals n . However, this is not always the case. When valence d , or f shells are filled, they may have relatively large overlap with the outermost core shell, which in these cases has the same principal quantum number. In Ref. [25] TEI corrections to the transitions frequencies of Ti^+ were found to be from 100 to 200 cm^{-1} . The ground configuration of Ti^+ is $3d^24s$ and the outermost core shell is $3p$. The $3d$ and $3p$ shells are not spatially separated and have significant overlap, resulting in the enhancement of the TEI contributions.

As we noted above, there is significant recent interest in HCI with optical transitions between the states of configurations with $4f$ and $5f$ electrons [11, 12]. Two very important experimental steps toward development of new frequency standards with these systems and subsequent application to the search for a possible variation of the fine-structure constant α were recently completed. First, predicted $5s - 4f$ transitions were detected in a number of HCI [26]. Second, sympathetic cooling of Ar^{13+} with Be^+ was demonstrated [27] paving the way to placing the highly-charged ions on the same footing as the singly-charged ions such as Al^+ currently used for optical atomic clocks [28].

Recent work [10] identified 10 HCI with very narrow optical transitions, where high precision spectroscopy is possible. All these ions have atomic cores with 46 electrons [$1s^2 \dots 4d^{10}$] and one to four valence electrons from the $4f$, $5s$, and $5p$ shells. Five ions from this list have three valence electrons: Ce^{9+} , Pr^{10+} , Nd^{11+} , Sm^{13+} , and Eu^{14+} . Their ground configurations are either $5s^25p$, or $5s^24f$. Pr^{9+} and Nd^{10+} have four valence electrons with ground state configurations $5s^25p^2$ and $5s^24f^2$, respectively. We expect that valence $4f$ orbitals have large overlap with the core shell $4d$, significantly enhancing three-particle interactions. Since prediction of accurate transition energies in these highly-charged ions is crucial for rapid experimental progress, it is important to evaluate the TEI contributions in these systems, which have been so far omitted in all relevant HCI calculations.

In this paper we study the role of such effective three-electron interactions in the spectra of polyvalent atoms and ions. Below we calculate TEI corrections to transition frequencies of the following ions: Ce^{9+} , $\text{Pr}^{9+,10+}$, $\text{Nd}^{10+,11+}$, Sm^{13+} , and Eu^{14+} . We also calculate properties of the U^{2+} ion as an example of the tetravalent system with the partially filled $5f$ shell [29]. We find that TEI corrections to the valence energies are typically of the order of few hundred cm^{-1} in these systems, but may exceed a thousand cm^{-1} . In some cases this is enough to change the order of low-lying levels significantly affecting theoretical predictions.

II. THEORY

We use Dirac-Coulomb-Breit Hamiltonian in the no-pair approximation [30, 31]. Low-lying levels of ions are found with the CI+AO method [23]. In this method, the core-valence and core-core correlations are treated using the linearized coupled-cluster method in the single-double approximation [32, 33] instead of the second order MBPT used in the CI+MBPT approach. A complete treatment of the TEI at the CI+AO level involves modification of the TEI diagrams in Fig. 1.c to the form presented in Fig. 2, where one Coulomb-Breit interaction is substituted by the respective cluster core-valence amplitude [22]. However, we find it sufficient to carry out CI+AO calculations of the wavefunctions and then treat TEI corrections within the second order MBPT for the systems of interest.

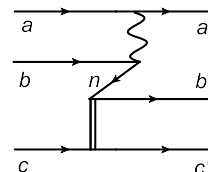


FIG. 2: The effective three-electron interaction in the coupled-cluster approximation. Double vertical line corresponds to the two-electron core-valence cluster amplitude. Such amplitudes are found by solving standard cluster equations [23]. Then, the TEI diagrams are evaluated using the resulting cluster amplitudes.

Our initial approximation corresponds to the Hartree-Fock potential of the core, V^{N_c} , where N_c is the number of core electrons. Such approximation completely neglects interactions between valence electrons and may be too crude for some neutral polyvalent atoms [24], but is sufficiently good for HCIs. Next, we form an effective Hamiltonian for valence electrons:

$$H_{\text{eff}}(E) = H_{\text{FC}} + \Sigma(E), \quad (1)$$

where H_{FC} is the Hamiltonian in the frozen-core approximation, which includes Coulomb-Breit interactions between valence electrons and the core potential V^{N_c} .

The energy-dependent operator $\Sigma(E)$ accounts for the core polarization effects, such as in Fig. 1.b. In the second order of MBPT this operator is a three-electron operator. In higher orders it is the N_v -electron operator, where N_v is the number of valence electrons (we assume that $N_v \geq 3$ and $N = N_c + N_v$ is the total number of electrons in the system). At this stage we neglect three-electron and many-electron interactions and consider operator Σ as a two-electron operator. Explicit expressions for Σ are given in Refs. [14, 23]. We use the Davidson algorithm to find L lowest eigenvalues and eigenfunctions of the operator H_{eff} (typically $L \sim 10$).

Selection rules for three-electron matrix elements are much weaker than for two-electron ones and the number

of nonzero matrix elements of the effective Hamiltonian drastically increases. Consequently, the matrix becomes less sparse. Forming and diagonalizing such matrix in a complete configurational space is impractically time-consuming. Instead, we include TEI by forming a small $L \times L$ matrix using eigenfunctions from the previous stage of the computation. Diagonalization of this matrix gives us eigenvalues with TEI corrections. This approach radically reduces the number of required three-electron diagrams without significant loss of accuracy.

III. RESULTS AND DISCUSSION

A. In-like and Sn-like HCI with narrow optical transitions

For In-like Ce^{9+} , Pr^{10+} , Nd^{11+} , Sm^{13+} , and Eu^{14+} ions (49 electrons) and for Sn-like Pr^{9+} and Nd^{10+} ions (50 electrons) we use the results of previous CI+AO calculations with Dirac-Coulomb-Breit two-electron effective Hamiltonian described in detail in Refs. [34] and [35] respectively. In-like ions were calculated in [34] in two approximations, either as systems with one, or three valence electrons. Similarly, Sn-like ions were treated in [35] as systems with two, or four valence electrons. Calculations with three and four valence electrons include correlations more completely and are expected to be more accurate. On the other hand, in these approximations we need to include TEI contributions. In this work, we use eigenfunctions obtained in [10, 34, 35] and add TEI corrections as discussed above.

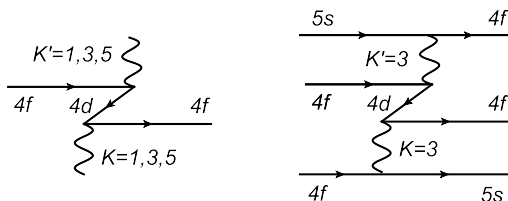


FIG. 3: TEI for the case of the valence $4f$ electron and the $4d$ core shell. Left panel: selection rules for the $4d$ - $4f$ vertex require odd multipoles K, K' for the Coulomb interaction. Right panel: example of the nonzero diagram for the configuration $5s4f^2$. Selection rules for the $5s^2 4f$ and $4f^3$ configurations require even multipoles and prohibit vertexes with $4d$ core shell electrons; thus, for these configuration the $4d$ contribution to TEI diagrams vanishes.

Trivalent ions considered in this work have the following low-lying valence configurations with $4f$ electrons: $5s^2 4f$, $5s4f^2$, and $4f^3$. Fig. 3 illustrates that the contribution from the uppermost $4d$ core shell in TEI diagrams vanishes for the $5s^2 4f$ and $4f^3$ configurations. Therefore, we can expect large TEI corrections only for the $5s4f^2$ configuration. In Ce^{9+} , Pr^{10+} , and Nd^{11+} this configuration lies very high and is not of interest to clock

applications. Only in Sm^{13+} this configuration is within the optical range transition from the ground configuration $5s^2 4f$. In Eu^{14+} the $5s4f^2$ configuration becomes the ground one. Consequently, the TEI corrections to the energies of the low-lying levels of Ce^{9+} , Pr^{10+} , and Nd^{11+} are rather small, but become much larger for Sm^{13+} and Eu^{14+} . For the former group of ions these corrections are on the order of 100 cm^{-1} or less, but for the latter group they exceed 500 cm^{-1} .

Results of our calculations for HCI with three valence electrons are presented in Table I. The spectrum of Eu^{14+} is also shown in the central panel of Fig. 4. The TEI corrections shift levels of the odd parity down by approximately 500 cm^{-1} , with the only exception of one level at the top of the plot. For this level there is large non-diagonal TEI interaction with the lower level of the same J and parity. This interaction is shown by the vertical arrow.

TABLE I: Calculated low-lying levels of Ce^{9+} , Pr^{10+} , Nd^{11+} , Sm^{13+} , and Eu^{14+} . Column 4 lists excitation energies in the CI+AO approximation from Ref. [34]. TEI corrections to the valence energy and respective shifts relative to the ground state are given in columns 5 and 6. Last column presents final calculated spectra. All values are in cm^{-1} .

Ion	Config.	J	CI+AO	TEI	Δ_{TEI}	Total
Ce^{9+}	$5s^2 5p$	$\frac{1}{2}$	0	171	0	0
	$5s^2 5p$	$\frac{3}{2}$	33436	177	6	33442
	$5s^2 4f$	$\frac{5}{2}$	55694	126	-45	55649
	$5s^2 4f$	$\frac{7}{2}$	58239	121	-50	58189
Pr^{10+}	$5s^2 5p$	$\frac{1}{2}$	0	183	0	0
	$5s^2 4f$	$\frac{3}{2}$	4496	147	-36	4460
	$5s^2 4f$	$\frac{5}{2}$	7817	141	-42	7776
	$5s^2 5p$	$\frac{3}{2}$	39127	190	7	39134
Nd^{11+}	$5s^2 4f$	$\frac{5}{2}$	0	167	0	0
	$5s^2 4f$	$\frac{7}{2}$	4173	160	-7	4167
	$5s^2 5p$	$\frac{1}{2}$	52578	198	31	52609
	$5s^2 5p$	$\frac{3}{2}$	97945	205	39	97984
Sm^{13+}	$5s^2 4f$	$\frac{5}{2}$	0	205	0	0
	$5s^2 4f$	$\frac{7}{2}$	6165	197	-8	6157
	$5s4f^2$	$\frac{11}{2}$	22521	530	326	22847
	$5s4f^2$	$\frac{13}{2}$	24774	531	326	25100
	$5s4f^2$	$\frac{13}{2}$	28135	527	322	28458
	$5s4f^2$	$\frac{15}{2}$	31470	528	324	31794
Eu^{14+}	$5s4f^2$	$\frac{7}{2}$	0	574	0	0
	$5s4f^2$	$\frac{9}{2}$	2592	575	1	2593
	$4f^3$	$\frac{7}{2}$	4235	-126	-700	3535
	$5s4f^2$	$\frac{11}{2}$	6694	569	-4	6690
	$4f^3$	$\frac{11}{2}$	8348	-115	-689	7659
	$5s4f^2$	$\frac{13}{2}$	9664	571	-3	9662
	$5s4f^2$	$\frac{13}{2}$	11259	565	-9	11250
	$5s4f^2$	$\frac{15}{2}$	11410	570	-3	11407
$4f^3$	$\frac{11}{2}$	12583	-110	-684	11900	

Tetravalent Pr^{9+} and Nd^{10+} ions have low-lying

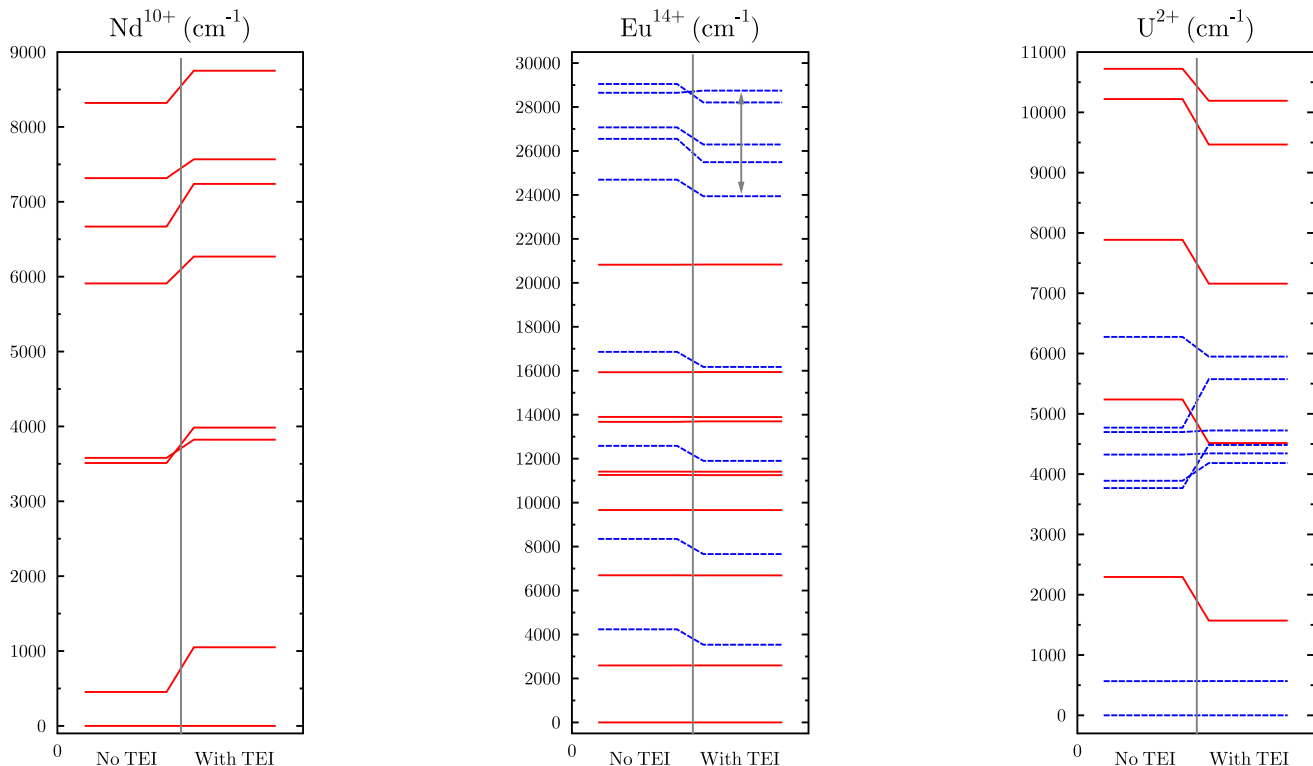


FIG. 4: (color online) Level diagrams of Nd^{10+} , Eu^{14+} , and U^{2+} ions with and without TEI corrections. Solid red lines – levels of even parity; dashed blue – odd parity. Vertical arrow in the central panel shows two strongly interacting levels.

TABLE II: Calculated low-lying levels of Pr^{9+} and Nd^{10+} (cm^{-1}). Notations are the same as in Table I.

Ion	Config.	J	CI+AO	TEI	Δ_{TEI}	Total
Pr^{9+}	$5s^2 5p^2$	0	0	571	0	0
	$5s^2 5p4f$	3	22918	544	-28	22891
	$5s^2 5p4f$	2	25022	874	303	25325
	$5s^2 5p4f$	3	28023	692	121	28143
	$5s^2 5p^2$	1	28422	606	34	28456
	$5s^2 5p4f$	4	30370	396	-175	30195
	$5s^2 5p^2$	2	36459	720	149	36607
	$5s^2 5p4f$	3	56234	869	298	56532
	Nd^{10+}	$5s^2 5p4f$	3	0	534	0
$5s^2 4f^2$		4	454	1115	581	1035
$5s^2 4f^2$		2	3580	828	293	3873
$5s^2 4f^2$		5	3512	1104	569	4081
$5s^2 5p4f$		3	5910	772	238	6147
$5s^2 4f^2$		6	6669	1093	559	7228
$5s^2 5p4f$		4	7316	698	164	7480
$5s^2 4f^2$		2	8320	975	441	8761

$5s^2 5p^2$, $5s^2 5p4f$, and $5s^2 4f^2$ configurations. There are no contributions of the uppermost core shell $4d$ to the TEI diagrams for the pure $5s^2 5p^2$ configuration. On the

other hand, the configuration interaction for these ions is stronger than for three electron ions and the $4d$ shell contributes even to those levels, which nominally belong to the $5s^2 5p^2$ configuration. Moreover, the number of permutations of the TEI diagrams for four-electron ions is larger leading to an additional enhancement of the TEI corrections. Our results are presented in Table II. Spectrum of Nd^{10+} is also shown in Fig. 4. We see that TEI corrections for all configurations are positive and large, on the order of 1000 cm^{-1} . Respective energy shifts relative to the ground state are significantly smaller, about 600 cm^{-1} , or less. We conclude that the size of TEI corrections for Pr^{9+} and Nd^{10+} is not so sensitive to the leading configuration and, therefore, is less predictable based on the selection rule arguments, since it is significantly affected by the configuration interaction.

B. The U^{2+} ion

In this section we consider U^{2+} as an example of an ion with the partially filled $5f$ shell. This ion has 4 valence electrons and the $[1s^2 \dots 5d^{10} 6s^2 6p^6]$ core. Low-lying configurations include $5f^3 6d$, $5f^3 7s$, and $5f^4$. Here, two valence orbitals have large overlap with the core: $5f$ overlaps with the $5d$ shell, while $6d$ overlaps with the $6p$

TABLE III: Calculated levels of U^{2+} (cm^{-1}). Eight lowest levels of each parity are listed. Notations are the same as in Table I.

Ion	Config.	J	CI+AO	TEI	Δ_{TEI}	Total
U^{2+}	$6d5f^3$	6	0	679	0	0
	$6d5f^3$	5	567	680	-13	568
	$5f^4$	4	2294	-45	-724	1571
	$6d5f^3$	3	3890	972	130	4184
	$5f^37s$	7	4324	698	80	4344
	$6d5f^3$	4	3769	1393	333	4483
	$5f^4$	5	5238	-44	-723	4515
	$6d5f^3$	6	4698	704	-181	4724
	$5f^37s$	5	4771	1482	145	5575
	$6d5f^3$	4	6276	352	304	5949
	$5f^4$	6	7886	-48	-727	7159
	$5f^4$	7	10221	-76	-755	9466
	$5f^4$	4	10722	149	-529	10192
	$5f^4$	3	11677	369	-309	11368
	$5f^4$	8	12345	-115	-794	11551
	$5f^4$	3	12660	355	-324	12336

shell. As a result, the TEI corrections are very large for the $5f^36d$ and $5f^37s$ configurations. For the $5f^4$ configuration selection rules for multipoles suppress the TEI corrections. We use results from Ref. [29] as a starting point for our calculation. In Table III we present the calculated spectrum of U^{2+} from Ref. [29] and our TEI corrections to the energies. Both spectra are also shown in the right panel of Fig. 4.

We see that TEI corrections in U^{2+} are large and significantly differ even for levels of the same configuration. This can be explained by the large number of diagrams for the four-electron system which can either add coherently or cancel each other. As expected, TEI corrections for the levels of the $5f^4$ configuration are several times smaller than for two other configurations due to selection rules.

The U^{2+} ion has the very dense spectrum with a typical level spacing of few hundred cm^{-1} even near the ground state. This is much smaller than the average TEI correction. Moreover, the dispersion of TEI corrections is also larger than the typical level spacing. Thus, it is not surprising that the order of levels appears to be significantly different when TEI corrections are taken into account (see the right panel of Fig. 4). We note, however, that TEI corrections are insufficient to significantly improve agreement between our theory and the experiment for U^{2+} .

C. Accuracy analysis

Let us briefly discuss how accurately we account for TEI interactions. Potentially there are three sources of errors:

(1) *Incompleteness of the one-electron basis set.* It is clear from Fig. 1.c that in TEI diagrams we do not sum over intermediate states (the only sum is over core states), so there is no error associated with the final basis set.

(2) *The truncation of the contributions from the subdominant configurations.* We neglect small contributions to the eigenfunctions when calculating TEI corrections. Typically, the configurational mixing accounts for 10% correction to the binding energy. Main part of this correction comes from the small number of leading configurations, which we take into account. We estimate the neglected part of this correlation correction to be on the order of 2 – 3% of the largest TEI correction.

(3) *High-order corrections to TEI diagrams.* We calculate TEI corrections within the second order MBPT, Fig. 1.c, instead of using more accurate expression Fig. 2. Higher-order terms typically give 5 – 10% corrections to the second order diagrams. As long as the cluster amplitudes in the diagram Fig. 2 are the same as in two-electron valence diagrams, we can expect similar size of the high-order corrections here, i.e. 5 – 10%.

We conclude that our error for the TEI contribution can be up to 10%. According to this estimate we can assign the TEI error bar to be 50 cm^{-1} for three-electron ions from Table I and about 100 cm^{-1} for four-electron ions from Table II. For U^{2+} both CI and high-order errors are the largest. We can assume here a conservative error bar of 200 cm^{-1} . All these error bars for TEI corrections are smaller than the total theoretical errors, so they do not affect the overall accuracy of the theory.

IV. CONCLUSIONS

We calculated corrections to the energies of several heavy polyvalent ions from the effective three-electron interactions induced by the core polarization. We find that these corrections may be on the order of 1000 cm^{-1} for systems with partially filled $4f$, or $5f$ shells. Atoms and ions with the partly filled f -shell usually have very dense spectrum and TEI corrections can change the predicted order of energy levels. Large TEI diagrams obey specific selection rules. For some configurations these selection rules cannot be satisfied suppressing the TEI corrections for levels of such configurations.

The number of TEI diagrams rapidly grows with the number of valence electrons and Hamiltonian matrix becomes less sparse. This makes it very difficult to account for TEI corrections accurately when they become large. Here we used relatively simple approximation when we calculated TEI corrections only in a small subspace spanned by lower eigenvectors of the unperturbed problem. This method works for the eigenvalues, but may be insufficient for other observables.

Finally, we note that ions considered here are sufficiently heavy for QED corrections to be important. In fact, QED corrections appear to be of the same order as

TEI corrections considered here. Therefore, accurate calculations have to account for both types of corrections. However, an accurate treatment of QED corrections in many-electron systems is highly non-trivial [36–39] and this topic is studied elsewhere [40].

Acknowledgments

This work is partly supported by Russian Foundation for Basic Research Grant No. 14-02-00241 and by U.S.

NSF Grants No. PHY-1404156 and No. PHY-1520993. One of us (IT) acknowledges support from Grant SPbSU No. 11.38.261.2014.

-
- [1] K. Tsigutkin, D. Dounas-Frazer, A. Family, J. E. Stal-
naker, V. V. Yashchuk, and D. Budker, *Phys. Rev. Lett.* **103**, 071601 (2009).
- [2] T. Pruttivarasin, M. Ramm, S. G. Porsev, I. I. Tupitsyn,
M. S. Safronova, M. A. Hohensee, and H. Häffner, *Nature*
(London) **517**, 592 (2015).
- [3] T. L. Nicholson, S. L. Campbell, R. B. Hutson, G. E.
Marti, B. J. Bloom, R. L. McNally, W. Zhang, M. D.
Barrett, M. S. Safronova, G. F. Strouse, et al., *Nature*
Communications **6**, 6896 (2015).
- [4] V. A. Dzuba, V. V. Flambaum, M. S. Safronova,
S. G. Porsev, T. Pruttivarasin, M. A. Hohensee, and
H. Häffner, *Nature Physics* **12**, 465 (2016).
- [5] M. Saffman and K. Mølmer, *Phys. Rev. A* **78**, 012336
(2008).
- [6] J. J. McClelland and J. L. Hanssen, *Phys. Rev. Lett.* **96**,
143005 (2006).
- [7] A. Cingöz, A. Lapiere, A. Nguyen, N. Leefler, D. Budker,
S. K. Lamoreaux, and J. R. Torgerson, *Phys. Rev. Lett.* **98**,
040801 (2007).
- [8] E. Paez, K. J. Arnold, E. Hajiyev, S. G. Porsev, V. A.
Dzuba, U. I. Safronova, M. S. Safronova, and M. D. Bar-
rett, *Phys. Rev. A* **93**, 042112 (2016).
- [9] V. A. Dzuba, M. S. Safronova, U. I. Safronova, and V. V.
Flambaum, *Phys. Rev. A* **92**, 060502 (2015).
- [10] M. S. Safronova, V. A. Dzuba, V. V. Flambaum, U. I.
Safronova, S. G. Porsev, and M. G. Kozlov, *Phys. Rev.*
Lett. **113**, 030801 (2014), arXiv:1405.4271.
- [11] J. C. Berengut, V. A. Dzuba, and V. V. Flambaum, *Phys.*
Rev. Lett. **105**, 120801 (2010), arXiv:1007.1068.
- [12] J. C. Berengut, V. A. Dzuba, V. V. Flambaum, and
A. Ong, *Phys. Rev. Lett.* **106**, 210802 (2011).
- [13] S. A. Maier and C. Honerkamp, *Phys. Rev. B* **85**, 064520
(2012), arXiv:1112.0229.
- [14] V. A. Dzuba, V. V. Flambaum, and M. G. Kozlov, *Phys.*
Rev. A **54**, 3948 (1996).
- [15] V. A. Dzuba, V. V. Flambaum, M. G. Kozlov, and S. G.
Porsev, *Sov. Phys.–JETP* **87**, 885 (1998).
- [16] M. G. Kozlov and S. G. Porsev, *Eur. Phys. J. D* **5**, 59
(1999).
- [17] M. G. Kozlov, S. G. Porsev, and W. R. Johnson, *Phys.*
Rev. A **64**, 052107 (2001), arXiv:physics/0105090.
- [18] I. M. Savukov and W. R. Johnson, *Phys. Rev. A* **65**,
042503 (2002).
- [19] V. A. Dzuba, *Phys. Rev. A* **71**, 032512 (2005).
- [20] V. A. Dzuba, *Phys. Rev. A* **71**, 062501 (2005).
- [21] I. M. Savukov, *Phys. Rev. A* **93**, 022511 (2016).
- [22] M. G. Kozlov, *Int. J. Quant. Chem.* **100**, 336 (2004),
arXiv:physics/0306061.
- [23] M. S. Safronova, M. G. Kozlov, W. R. Johnson,
and D. Jiang, *Phys. Rev. A* **80**, 012516 (2009),
arXiv:0905.2578.
- [24] S. G. Porsev, M. G. Kozlov, M. S. Safronova, and
I. I. Tupitsyn, *Phys. Rev. A* **93**, 012501 (2016),
arXiv:1510.06679.
- [25] J. C. Berengut, V. V. Flambaum, and M. G. Kozlov, *J.*
Phys. B **41**, 235702 (2008), arXiv:0806.3501.
- [26] A. Windberger, J. R. C. López-Urrutia, H. Bekker, N. S.
Oreshkina, J. C. Berengut, V. Bock, A. Borschevsky,
V. A. Dzuba, E. Eliav, Z. Harman, et al., *Phys. Rev.*
Lett. **114**, 150801 (2015).
- [27] L. Schmöger, O. O. Versolato, M. Schwarz, M. Kohnen,
A. Windberger, B. Piest, S. Feuchtenbeiner,
J. Pedregosa-Gutierrez, T. Leopold, P. Micke, et al.,
Science **347**, 1233 (2015).
- [28] C. W. Chou, D. B. Hume, J. C. J. Koelemeij, D. J.
Wineland, and T. Rosenband, *Phys. Rev. Lett.* **104**,
070802 (2010).
- [29] I. Savukov, U. I. Safronova, and M. S. Safronova, *Phys.*
Rev. A **92**, 052516 (2015).
- [30] J. Sucher, *Phys. Rev. A* **22**, 348 (1980).
- [31] L. N. Labzowsky, G. L. Klimchitskaia, and Y. Y.
Dmitriev, *Relativistic effects in the spectra of atomic sys-*
tems (CRC Press, 1993), ISBN 0750302232.
- [32] S. A. Blundell, W. R. Johnson, and J. Sapirstein, *Phys.*
Rev. A **43**, 3407 (1991).
- [33] M. S. Safronova, W. Johnson, and A. Derevianko, *Phys.*
Rev. A **60**, 4476 (1999).
- [34] M. S. Safronova, V. A. Dzuba, V. V. Flambaum, U. I.
Safronova, S. G. Porsev, and M. G. Kozlov, *Phys. Rev.*
A **90**, 042513 (2014), arXiv:1407.8272.
- [35] M. S. Safronova, V. A. Dzuba, V. V. Flambaum, U. I.
Safronova, S. G. Porsev, and M. G. Kozlov, *Phys. Rev.*
A **90**, 052509 (2014), arxiv:1409.6124.
- [36] V. V. Flambaum and J. S. Ginges, *Phys. Rev. A* **72**,
052115 (2005).
- [37] V. M. Shabaev, I. I. Tupitsyn, and V. A. Yerokhin, *Phys.*
Rev. A **88**, 012513 (2013).
- [38] V. Shabaev, I. Tupitsyn, and V. Yerokhin, *Computer*
Physics Communications **189**, 175 (2015).
- [39] J. S. M. Ginges and J. C. Berengut, *J. Phys. B* **49**, 095001
(2016), arXiv:1511.01459.
- [40] I. I. Tupitsyn, M. G. Kozlov, M. S. Safronova, V. M.
Shabaev, and V. A. Dzuba, arXiv:1607.07064 (2016).